energy&fuels

Article

Cite This: Energy Fuels 2019, 33, 2301−2307

pubs.acs.org/EF

Sewage Sludge Gasification under a Hydrothermal Condition: Phosphorus Behavior and Its Kinetics

Apip Amrullah[†,‡] and Yukihiko Matsumura*[,†]

[†]Department of Mechanical Science and Engineering, Hiroshima University, 1-4-1 Kagamiyama, Higashi-Hiroshima 739-8527, Japan

[‡]Department of Mechanical Engineering, Lambung Mangkurat University, Banjarmasin 70123, South Kalimantan, Indonesia

ABSTRACT: This is the first report to model the behavior of phosphorus in sewage sludge under a hydrothermal condition for the ranges of temperature 300−600 °C and reaction time 5−30 s using a continuous reactor. The pressure was fixed at 25 MPa. H_2, CO_2, and CH_4 were components of the product gas. At the short reaction time of less than 10 s, organic phosphorus (OP) was almost completely converted to inorganic phosphorus (IP) under supercritical conditions. Then, a part of IP precipitated in the reactor. Kinetics parameters for the reaction from OP to IP were determined by assuming the first-order reaction. The precipitation rate in proportion to oversaturation fitted the experimental data well.

1. INTRODUCTION

Fossil fuels are limited-vitality energy sources, and their utilization is related to environmental issues. These problems have driven researchers to develop renewable energy technologies including gasification of biomass. A type of potential biomass that is a low-cost material and available in a large amount is sewage sludge. Sewage sludge contains a large amount of organic matter,[1] nitrogen, and phosphorus. Thus, sewage sludge can be utilized to generate gas for energy, as well as to recover phosphorus that is also a valuable commodity material. In pioneering studies, Adam et al.[3] found that P bioavailability was considerably inflated throughout the thermochemical treatment. Unfortunately, sewage sludge has high water content. The challenge of exploitation of biomass with high water content is that predrying is often needed for the most ancient thermochemical treatment method to recover energy.[2]

Meanwhile, the technology of sub- and supercritical water gasification utilizes water as the medium where various reactions of biomass can take place. The term "supercritical" denotes the region of temperature on the far side of the critical point, i.e., 374 °C. Under this condition, the hydrogen bonding between molecules in water weakens and contributes to H_2 production.[4,5] In distinction, the term "subcritical" denotes the region of the temperature higher than 100 °C and less than the critical temperature (374 °C) with high pressure (5−22 MPa). Under the subcritical condition, the liquid state of water is maintained.[6] Recent works of supercritical water gasification (SCWG)[7−11] demonstrated that under the supercritical water condition all of the fluids become one phase. Therefore, water is a suitable solution for organic materials and gaseous products. The gasification reaction of wet biomass in water can be carried out using SCWG, and the predrying process can be abolished.[12]

Studies on SCWG of sewage sludge, focusing on gas production, have been carried out. Supercritical water has been confirmed to be able to convert SS into H_2, CO, and CH_4 with the less solid product than that of traditional thermal processes.[13] Another study reported that using a high-pressure autoclave the effect of chemical composition on gas production was reported. At the higher reactant composition, the total gas production increased.[14] Also, Reddy et al.[15] pointed out that the gasification efficiency was affected by the feed biomass concentration.

Sewage sludge contains a high amount of phosphorus that makes it an important resource for phosphorus recovery. Phosphorus has been produced using traditional techniques as a marketable product, like mineral plant food, fodder, pure type of phosphorus, and phosphoric acid.[16] Therefore, a deeper understanding of P recovery from sewage sludge is necessary. Several studies have been recently performed concerning phosphorus recovery from sewage sludge. As reported by Yuan et al.,[17] the EBPR method is an attractive method for phosphorus recovery from wastewater treatment. Arakane et al.[18] reported that under the subcritical water condition magnesium ammonium phosphate (MAP) crystallization is a common technique for phosphorus recovery in excess sludge. Most recently, Zou and Wang[19] claimed that crystallization as hydroxyapatite (HAP) is often used for phosphorus recovery in domestic wastewater. These results show that the recovery rate of total phosphorus was 0.593 mol/mol. The removal efficiencies were 0.826, 0.875, and 0.916 for COD, PO_4^{3-}-P, and NO_3-N, respectively.

Considering that sub- or supercritical water gasification gasifies organics, leaving phosphorus behind, this technology should be effective for phosphorus recovery in sewage sludge. It is also critical for energy generation from sewage sludge because inorganic removal results in no production of ash to plug the reactor. In addition, phosphorus recovery helps improving the economic aspect of the process by value added by-product formation. However, as far as we know, studies on phosphorus behavior combined with gas generation as well as the reaction kinetics of P transformation of sewage sludge under the hydrothermal condition are still limited. This

Received: December 11, 2018
Revised: February 20, 2019
Published: February 20, 2019

DOI: 10.1021/acs.energyfuels.8b04289
Energy Fuels 2019, 33, 2301−2307

Table 1. Proximate and Ultimate Analysis[a]

	proximate analysis [kg/kg-dry]			ultimate analysis [kg/kg-dry] (wt/wt, dry base)					
water content [kg/kg-wet]	VM	FC	Ash	C	H	N	S	O	P
0.792	0.775	0.580	0.167	0.431	0.066	0.044	0.024	0.259	0.013

[a]VM, volatile matter; FC, fixed carbon; C, carbon; H, hydrogen; N, nitrogen; S, Sulfur; O, oxygen.

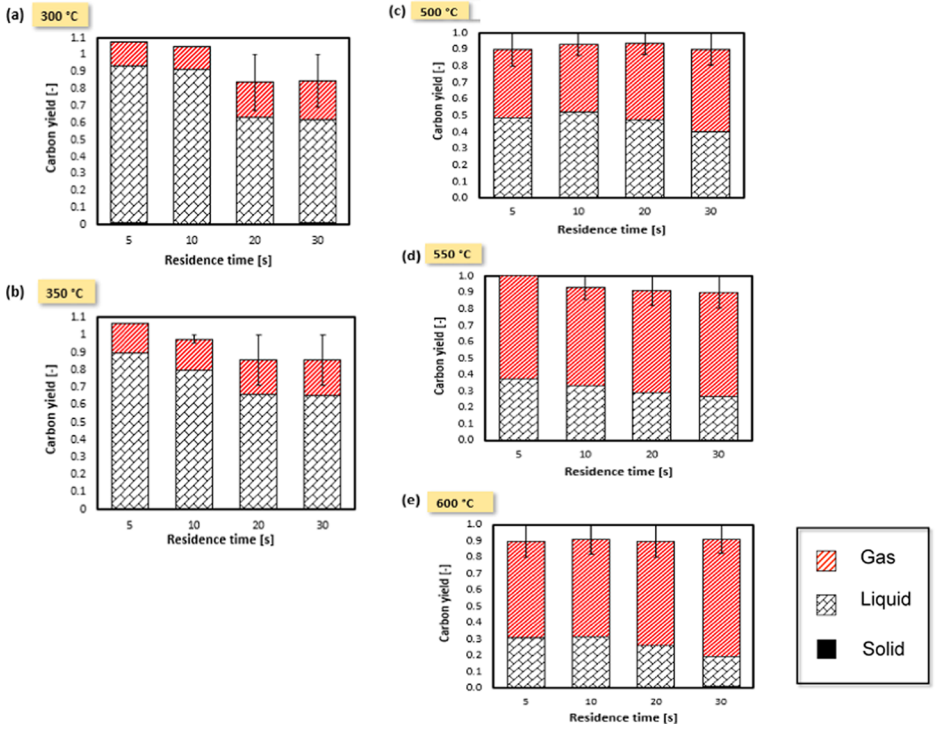

Figure 1. Carbon balance: carbon in the liquid, solid, and gas products: (a) 300 °C, (b) 350 °C, (c) 500 °C, (d) 550 °C, and (e) 600 °C. The data for 500, 550, and 600 °C are taken from Amrullah and Matsumura.[20]

information should be important for the phosphorus regeneration process from sewage sludge using sub- or supercritical water. Thus, we herein aim to elucidate the behavior of phosphorus together with sewage sludge gasification characteristics and determine the kinetics of phosphorus change during hydrothermal gasification.

2. MATERIALS AND METHODS

2.1. Feedstock. The sewage sludge in this work was the same as the one previously reported.[20] Briefly, it was active sludge produced from the Higashi-Hiroshima wastewater treatment plant. The particle size of 40 μm was obtained after the pulverization process. The properties of the sewage sludge were obtained by our research group[21] as shown in Table 1. A water deionizer (Organo, BB-5A) produced deionized water (<1 μS/cm) to be used here.

2.2. Experimental Details. Using a continuous reactor, sewage sludge was gasified in not only subcritical water but also the supercritical water region. We have already reported the details of the reactor.[20] The reactor was made from stainless steel 316 with an inner diameter of 2.17 mm (an outer diameter is 3.18 mm) and a length of 12 m and was heated by an electric furnace. While flowing water at 25 MPa, the constant desired temperature was achieved with the electric furnace. Then, feedstock was fed into the system. After waiting for 1 h for the steady-state condition, sample collection was made for gas and liquid effluent.

To cool down the reactor, water was fed into the reactor, resulting in part of phosphorus precipitated in the reactor recovered for collection and analysis.

The reaction temperature was changed as 300, 350, 500, 550, and 600 °C. The residence time was changed from 5 to 30 s. Calculation to obtain the residence time has been introduced in our previous study.[20]

2.3. Analytical Method. The details of the analysis employed in this work are presented elsewhere.[20] Briefly, the rate of gas generation was determined on the basis of the gas collection time to fill the 14 cm^3 sampling bottle with the gas. After experimental runs, gas was sampled and analyzed by gas chromatography (GC). By using a TOC analyzer, the carbon content in the liquid phase was determined. To measure the phosphate ion in the liquid phase, an ion chromatography (IC) analyzer was used. To measure the total phosphorus (TP) amount, the molybdenum blue methodology was the successful application. The equations to determine IP and TP yields in this study are presented elsewhere.[20]

The calculation of carbon gasification efficiency (CGE) in this study was done by eq 1, where C_{gas}, C_{IC}, and $C_{feedstcok}$ denote carbon amount in the gas product [mol], liquid product [mol], and the sewage sludge [mol], respectively.

$$\mathrm{CGE} = \frac{C_{gas} + C_{IC}}{C_{feedstock}} \quad (1)$$

The measurement was conducted thrice, and the average was taken.

3. RESULTS AND DISCUSSION

Figure 1 shows the product carbon distribution in gas and liquid after all experimental runs. Carbon balance higher than 0.8 was obtained for each condition. The carbon yield of gas increases rapidly with temperature. This is the typical behavior

DOI: 10.1021/acs.energyfuels.8b04289
Energy Fuels 2019, 33, 2301−2307

observed in the SCWG process. The temperature exceeding the critical point (374 °C) gives the increase of gaseous products, as observed by Paksung and Matsumura.[9] As mentioned by another previous work,[22,23] higher gas yield was obtained when the temperature was higher than the critical value due to the reduced ionic product and the decreased water density.

Table 2 shows the CGE of sewage sludge at varies temperatures and residence times. It clearly shows that the high temperature and long residence time resulted in high CGE. This is the widely recognized characteristics of hydrothermal gasification.[24−27] At temperatures above 500 °C, the effect of the residence time may look to be insignificant, showing a smaller increase in the CGE. This should be due to the characteristics of the first-order reaction. A higher temperature results in a higher conversion, where unreacted feedstock becomes less and the increase in the CGE becomes small.

Table 2. CGE Results at Different Temperatures and Residence Times

	temperature [°C] CGE [−]				
residence time [s]	300	350	500	550	600
5	0.14	0.17	0.41	0.63	0.59
10	0.14	0.18	0.41	0.60	0.60
20	0.21	0.20	0.46	0.62	0.64
30	0.23	0.21	0.50	0.64	0.72

Figure 2 shows the corresponding gas composition. Under the subcritical condition, it can be clearly seen in Figure 2a,b that H_2 and CO_2 were obtained as the major gas products. CH_4 and C_2H_4 were obtained in a small quantity, and no CO was found. This result agrees well with a previous publication by Seif et al.,[27] who showed that CO was a negligible amount of distillery wastewater treatment in subcritical water gasification. In the SCWG regime, the temperature has more effect on product gas composition. Figure 2c,d shows gas compositions for supercritical water conditions. H_2, CO_2, and CH_4 are main gaseous products under SCWG, and small amounts of C_2H_4 and C_2H_6 were also obtained. The level of CO was negligible. This result agrees with a previous work,[25,28] where no CO was obtained using humic acid. Most recently, Castello et al.[29] concluded that water−gas shift and methanation reactions had an important role in the gas-phase species, where CO was a reactive gas.[30]

At 330−350 °C, CO_2 was obtained as the main gas product. The decarboxylation reaction should have taken place. This result agrees with prior studies,[31−34] where at a lower temperature the decarboxylation reaction occurred. At a higher temperature (500−550 °C), the water−gas shift reaction took place in addition to the thermal decomposition of intermediate compounds, resulting in H_2 production as the key product in a short time. At all temperatures and a longer residence time, the methanation reaction proceeded, causing the CH_4 increase. This result agrees well with another previous work.[35] Overall, this result trend goes along with those of Wilkinson et al.[36] and Matsumura et al.,[37] i.e., temperature has affected the gasification rate of biomass. Sewage sludge is thus usual gasification feedstock and its behavior is predictable and controllable in this sense.

3.1. Behavior of Phosphorus. Figure 3 shows the phosphorus yield after sub- and supercritical water gasification. Figure 3a,b displays the phosphorus yield under the subcritical condition. The residence time affects the OP and IP behavior. The yield of OP decreases, whereas the yield of IP increases. Apparently, OP is converted to IP under the hydrothermal condition. This result shows good agreement with that of Zhu

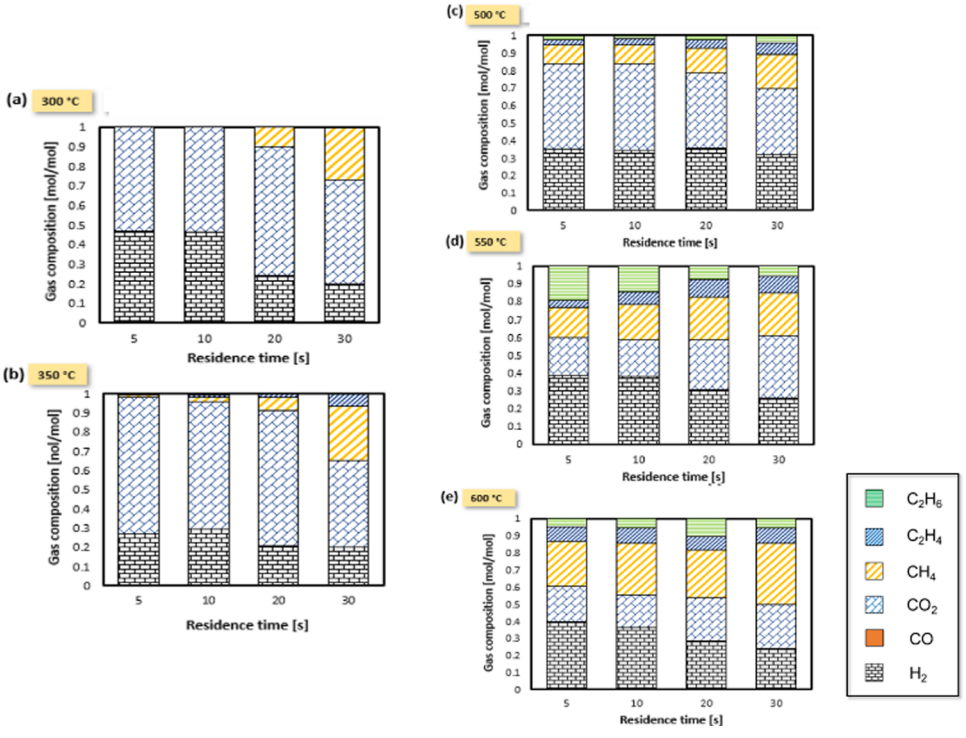

Figure 2. Gas composition for each condition: (a) 300 °C, (b) 350 °C, (c) 500 °C, (d) 550 °C, and (e) 600 °C. The data for 500, 550, and 600 °C are taken from Amrullah and Matsumura.[20]

DOI: 10.1021/acs.energyfuels.8b04289
Energy Fuels 2019, 33, 2301−2307

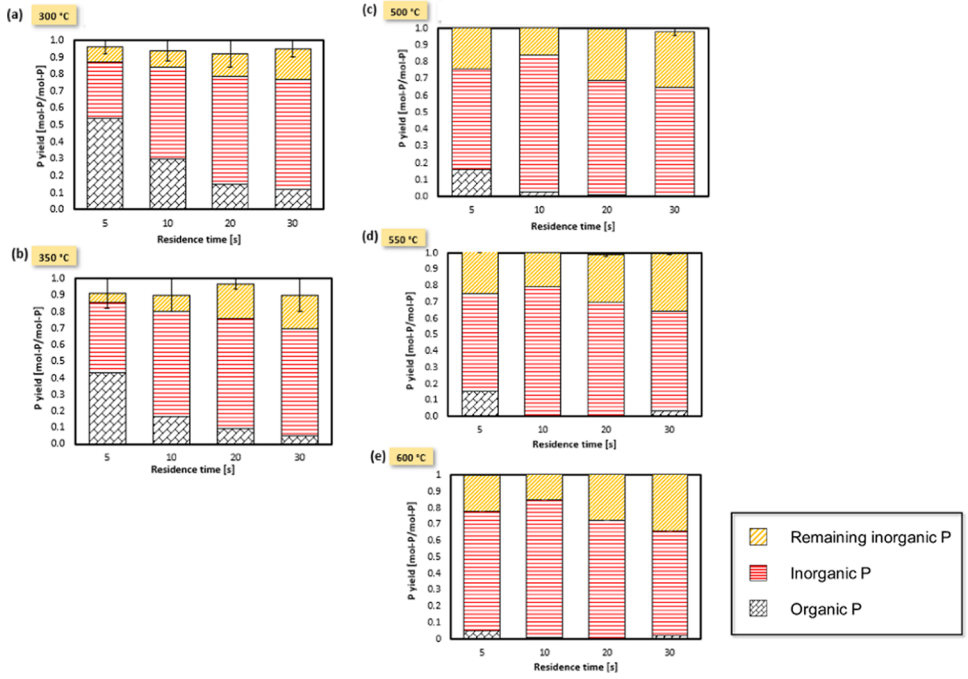

Figure 3. Phosphorus yield obtained in this study for each experimental condition: (a) 300 °C, (b) 350 °C, (c) 500 °C, (d) 550 °C, and (e) 600 °C. The data for 500, 550, and 600 °C are taken from Amrullah and Matsumura.[20]

et al.,[21] who found that at a longer reaction time OP was completely converted using an autoclave reactor.

Figure 3c–e shows that OP yield also decreases with a residence time in the supercritical region but more rapidly. IP yield increases in correspondence to this OP decrease, but for a longer residence time, a decrease in IP yield is observed, leading to an increase in the yield of remaining IP. The conversion of OP is approximate 99% when the residence time was 10 s and the temperature is high. Supercritical water shows the low solubility of salt, which must have caused the precipitation of the IP product.

Reaction kinetics for phosphorus behavior was modeled as follows. The overall change of phosphorus is as follows.

$$\mathrm{OP} \rightarrow \mathrm{IP} \rightarrow (\text{remaining IP}) \tag{2}$$

Conversion of OP to IP should be associated with the decomposition of organic compounds. Assumption of a first-order reaction should be natural. Conversion of IP in the liquid phase to remaining IP is precipitation. This rate is zero when the liquid-phase IP concentration [IP] is lower than the saturated IP concentration $[\mathrm{IP}]_0$, and when more IP is accumulated in the liquid phase, [IP] becomes greater than $[\mathrm{IP}]_0$ and it can be in proportion to the oversaturation, $[\mathrm{IP}] - [\mathrm{IP}]_0$. It is also noted that integration of this precipitation rate gives the amount of remaining IP and that the sum of the yields of OP, IP, and remaining IP should be unity. Taking into account that yields of liquid-phase products are in proportion with the liquid-phase concentration of the product, the following sets of equations are obtained.

$$\frac{dY(\mathrm{OP})}{dt} = -k_1 Y(\mathrm{OP}) \tag{3}$$

$$\frac{dY(\text{remaining IP})}{dt} = 0 \quad (0 < t < t') \tag{4}$$

$$\frac{dY(\text{remaining IP})}{dt} = k_2[Y(\mathrm{IP}) - Y(\mathrm{IP}_0)] \quad (t \geq t') \tag{5}$$

$$1 = Y(\mathrm{OP}) + Y(\mathrm{IP}) + Y(\text{remaining IP}) \tag{6}$$

where $Y(X)$ denotes the yield of X, but $Y(\mathrm{IP}_0)$ denotes the liquid-phase inorganic phosphorus yield that corresponds to the saturated concentration of inorganic phosphorus, k_1 and k_2 denote constants, and t' denotes the time when [IP] becomes equal to $[\mathrm{IP}]_0$.

Integrating eq 3 gives

$$Y(\mathrm{OP}) = \exp(-k_1 t) \tag{7}$$

While $Y(\mathrm{IP})$ is less than $Y(\mathrm{IP}_0)$ or $0 < t < t'$,

$$Y(\mathrm{IP}) = 1 - \exp(-k_1 t) \tag{8}$$

$$Y(\text{remaining IP}) = 0 \tag{9}$$

Thus,

$$Y(\mathrm{IP}_0) = 1 - \exp(-k_1 t') \tag{10}$$

When $Y(\mathrm{IP})$ is greater than $Y(\mathrm{IP}_0)$ or $t \geq t'$, eq 6 gives the following.

$$1 = \exp(-k_1 t) + Y(\mathrm{IP}) + \int_{t'}^{t} k_2[Y(\mathrm{IP}) - Y(\mathrm{IP}_0)]\, dt \tag{11}$$

By differentiating this equation in terms of t, we obtain

$$-k_1 \exp(-k_1 t) + \frac{dY(\mathrm{IP})}{dt} + k_2[Y(\mathrm{IP}) - Y(\mathrm{IP}_0)] = 0 \tag{12}$$

This differential equation can be solved with the boundary condition

$$t = t' \colon Y(\mathrm{IP}) = Y(\mathrm{IP}_0) \tag{13}$$

and the following solution can be obtained.

DOI: 10.1021/acs.energyfuels.8b04289
Energy Fuels 2019, 33, 2301−2307

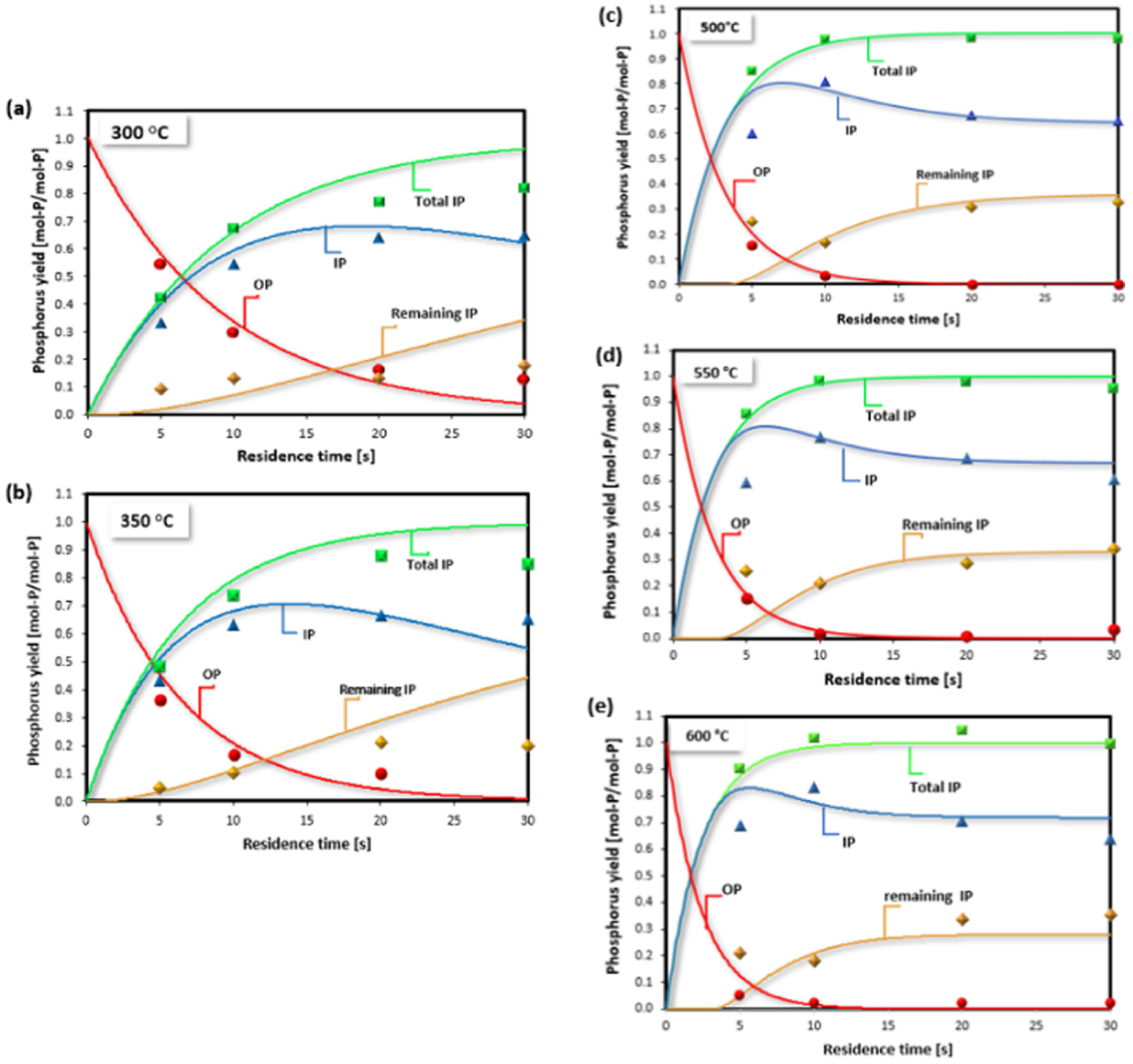

Figure 4. Phosphorus behavior of sewage sludge under sub- and supercritical water conditions at (a) 300 °C, (b) 350 °C, (c) 500 °C, (d) 550 °C, and (e) 600 °C. The symbols represent the experimental data, and the solid lines represent the calculated data. The data for (c), (d), and (e) are taken from Amrullah and Matsumura.[20]

$$Y(\mathrm{IP}) = \frac{k_1 \exp(-k_1 t) - k_2 \exp(-k_1 t' - k_2(t - t'))}{k_2 - k_1} + \exp(-k_2(t - t')) + [1 - \exp(-k_2(t - t'))]Y(\mathrm{IP}_0) \quad (14)$$

Finally,

$$Y(\text{remaining IP}) = 1 - Y(\mathrm{OP}) - Y(\mathrm{IP}) \quad (15)$$

Substituting eq 7 and eq 14 into eq 15 gives

$$Y(\text{remaining IP}) = 1 - \frac{k_2}{k_2 - k_1}[\exp(-k_1 t) - \exp(-k_1 t' - k_2(t - t'))] - \exp(-k_2(t - t')) - [1 - \exp(-k_2(t - t'))]Y(\mathrm{IP}_0) \quad (16)$$

The constant parameters k_1, k_2, and $Y(\mathrm{IP}_0)$ were determined. The LSE method and nonlinear regression were employed in this study.

Figure 4 shows the experimental and calculated yields of OP, IP, and remaining IP. The calculated yield is shown as a solid line. The comparison between experimental data for phosphorus yield and calculated values is depicted in Figure 5.

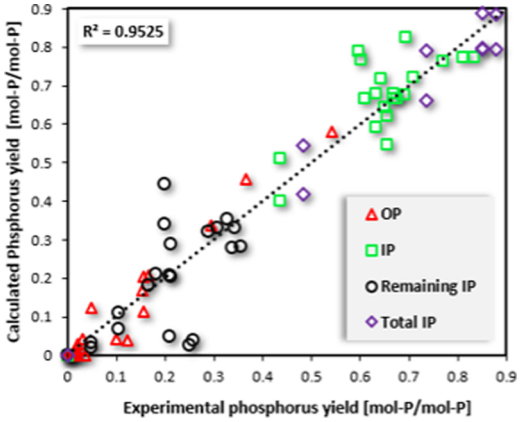

Figure 5. Parity plot of P yield in sub- and supercritical water gasification of sewage sludge (temp., 300−600 °C; 25 MPa; and SS concentration, 0.1 wt %).

The calculated conversion of OP during hydrothermal gasification of sewage sludge fitted well with the experimental

DOI: 10.1021/acs.energyfuels.8b04289
Energy Fuels 2019, 33, 2301−2307

data. Thus, obtained parameters are presented in Table 3. It is to be noted that for the parameters associated with precipitation, k_2 and $Y(IP_0)$ show a large difference between supercritical and subcritical values. Considering the large change in physical characteristics of water at a critical point, this phenomenon may be understandable.

Table 3. Constant Parameters Obtained from the First-Order Reaction Model for Sewage Sludge Conversion under Sub- and Supercritical Condition

	temperature [°C]				
constant parameters	300	350	500	550	600
k_1 [s^{-1}]	0.119	0.157	0.316	0.356	0.416
k_2 [s^{-1}]	0.023	0.028	0.208	0.267	0.358
Y (IP_0) [−]	0.0631	0.0565	0.642	0.667	0.719

The Arrhenius plot was taken for the constant parameter associated with the reaction, k_1, as shown in Figure 6. A good straight line was obtained. The activation energy (E_a) was 18.5 kJ mol^{-1}, and the value of the pre-exponential factor (A) was 5.4 s^{-1}.

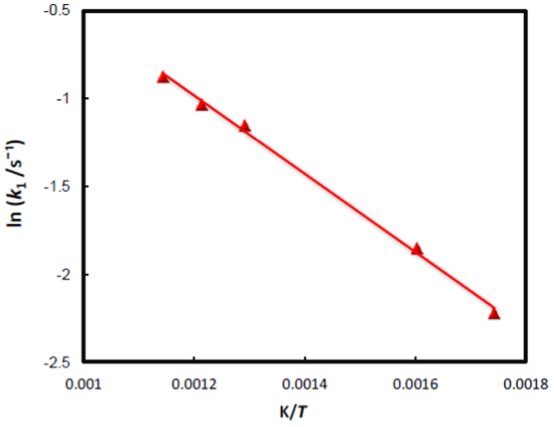

Figure 6. Arrhenius plot for the reaction rate constant of OP → IP under sub- and supercritical water conditions (temperature range of 300−600 °C, 25 MPa, and SS concentration 0.1 wt %).

4. CONCLUSIONS

The behavior of phosphorus during hydrothermal gasification at various temperatures and residence times was investigated for the first time. At the short residence time (10 s), OP was converted into IP quickly and then part of IP was precipitated in the reactor. The conversion of OP to IP model assuming the first-order reaction and the precipitation rate in proportion to oversaturation was proposed and the calculation based on this fitted the experimental data well.

AUTHOR INFORMATION

Corresponding Author

*E-mail: mat@hiroshima-u.ac.jp. Tel: +81-82-424-7561. Fax: +81-82-422-7193.

ORCID

Yukihiko Matsumura: 0000-0002-1341-0493

Notes

The authors declare no competing financial interest.

ACKNOWLEDGMENTS

A.A. received the financial support from the LPDP Scholarship. Supports from the Higashi-Hiroshima Wastewater Treatment Center and Tanikawa Fund are highly appreciated.

REFERENCES

(1) Moon, J.; Mun, T. Y.; Yang, W.; Lee, U.; Hwang, J.; Jang, E.; et al. Effects of hydrothermal treatment of sewage sludge on pyrolysis and steam gasification. *Energy Convers. Manage.* **2015**, *103*, 401−7.

(2) Furness, D. T.; Hoggett, L. A.; Judd, S. J. Thermochemical treatment of sewage sludge. *Water Environ. J.* **2002**, 57−65.

(3) Adam, C.; Peplinski, B.; Michaelis, M.; Kley, G.; Simon, F. G. Thermochemical treatment of sewage sludge ashes for phosphorus recovery. *Waste Manage.* **2009**, *29*, 1122−8.

(4) Nanda, S.; Reddy, S. N.; Dalai, A. K.; Kozinski, J. A. Subcritical and supercritical water gasification of lignocellulosic biomass impregnated with nickel nanocatalyst for hydrogen production. *Int. J. Hydrogen Energy* **2016**, *41*, 4907−21.

(5) Li, H.; Chen, Z.; Huo, C.; Hu, M.; Guo, D.; Xiao, B. Effect of bioleaching on hydrogen-rich gas production by steam gasification of sewage sludge. *Energy Convers. Manage.* **2015**, *106*, 1212−8.

(6) Hassas-Roudsari, M.; Chang, P. R.; Pegg, R. B.; Tyler, R. T. Antioxidant capacity of bioactives extracted from canola meal by subcritical water, ethanolic and hot water extraction. *Food Chem.* **2009**, *114*, 717−26.

(7) Kruse, A.; Dinjus, E. Hot compressed water as reaction medium and reactant. 2. Degradation reactions. *J. Supercrit. Fluids* **2007**, *41*, 361−79.

(8) Yanagida, T.; Minowa, T.; Nakamura, A.; Matsumura, Y.; Noda, Y. Behavior of inorganic elements in poultry manure during supercritical water gasification. *J. Jpn. Inst. Energy* **2008**, *87*, 731−6.

(9) Paksung, N.; Matsumura, Y. Decomposition of Xylose in Sub- and Supercritical Water. *Ind. Eng. Chem. Res.* **2015**, *54*, 7604−13.

(10) Samanmulya, T.; Farobie, O.; Matsumura, Y. Gasification Characteristics of Aminobutyric Acid and Serine as Model Compounds of Proteins under Supercritical Water Conditions. *J. Jpn. Pet. Inst.* **2017**, *60*, 34−40.

(11) Matsumura, Y.; Minowa, T.; Potic, B.; Kersten, S. R. A.; Prins, W.; Van Swaaij, W. P. M.; et al. Biomass gasification in near- and super-critical water: Status and prospects. *Biomass Bioenergy* **2005**, *29*, 269−92.

(12) Farobie, O.; Changkiendee, P.; Inoue, S.; Inoue, T.; Kawai, Y.; Noguchi, T.; et al. Effect of the Heating Rate on the Supercritical Water Gasification of a Glucose/Guaiacol Mixture. *Ind. Eng. Chem. Res.* **2017**, *56*, 6401−7.

(13) Zhang, L.; Charles, X. C.; Champagne, P. Energy recovery from secondary pulp/paper-mill sludge and sewage sludge with supercritical water treatment. *Bioresour. Technol.* **2010**, *101*, 2713−21.

(14) Gong, M.; Zhu, W.; Fan, Y.; Zhang, H.; Su, Y. Influence of the reactant carbon-hydrogen-oxygen composition on the key products of the direct gasification of dewatered sewage sludge in supercritical water. *Bioresour. Technol.* **2016**, *208*, 81−6.

(15) Reddy, S. N.; Nanda, S.; Dalai, A. K.; Kozinski, J. A. Supercritical water gasification of biomass for hydrogen production. *Int. J. Hydrogen Energy* **2014**, *39*, 6912−26.

(16) Egle, L.; Rechberger, H.; Krampe, J.; Zessner, M. Phosphorus recovery from municipal wastewater: An integrated comparative technological, environmental and economic assessment of P recovery technologies. *Sci. Total Environ.* **2016**, *571*, 522−42.

(17) Yuan, Z.; Pratt, S.; Batstone, D. J. Phosphorus recovery from wastewater through microbial processes. *Curr. Opin. Biotechnol.* **2012**, *23*, 878−83.

(18) Arakane, M.; Imai, T.; Murakami, S.; Takeuchi, M. Resource Recovery from Excess Sludge by Subcritical Water Process with Magnesium Ammonium Phosphate Process. *J. Water Environ. Nanotechnol.* **2005**, *3*, 119.

(19) Zou, H.; Wang, Y. Phosphorus removal and recovery from domestic wastewater in a novel process of enhanced biological

DOI: 10.1021/acs.energyfuels.8b04289
Energy Fuels 2019, 33, 2301−2307

phosphorus removal coupled with crystallization. *Bioresour. Technol.* **2016**, *211*, 87−92.
(20) Amrullah, A.; Matsumura, Y. Supercritical water gasification of sewage sludge in continuous reactor. *Bioresour. Technol.* **2018**, *249*, 276−83.
(21) Zhu, W.; Xu, Z. R.; Li, L.; He, C. The behavior of phosphorus in sub- and super-critical water gasification of sewage sludge. *Chem. Eng. J.* **2011**, *171*, 190−6.
(22) Promdej, C.; Chuntanapum, A.; Matsumura, Y. Effect of temperature on tarry material production of glucose in supercritical water gasification. *J. Jpn. Inst. Energy* **2010**, *89*, 1179−84.
(23) Unami, Y.; Kanna, M.; Yanagida, T.; Matsumura, Y. Phosphorus Recovery by Supercritical Water Gasification of Sewage Sludge, Pa-216, In: Proceedings of the 8th Conference on Biomass Science, Higashi-Hiroshima, Jan. 9−10, 2013, Higashi-Hiroshima, Japan (in Japanese), 2013.
(24) Guo, Y.; Wang, S. Z.; Xu, D. H.; Gong, Y. M.; Ma, H. H.; Tang, X. Y. Review of catalytic supercritical water gasification for hydrogen production from biomass. *Renewable Sustainable Energy Rev.* **2010**, *14*, 334−43.
(25) Lee, M.; Kim, D. Journal of Industrial and Engineering Chemistry Identi fi cation of phosphorus forms in sewage sludge ash during acid pre-treatment for phosphorus recovery by chemical fractionation and spectroscopy. *J. Ind. Eng. Chem.* **2017**, *51*, 64−70.
(26) Lim, B. H.; Kim, D. J. Selective acidic elution of Ca from sewage sludge ash for phosphorus recovery under pH control. *J. Ind. Eng. Chem.* **2017**, *46*, 62−7.
(27) Seif, S.; Tavakoli, O.; Fatemi, S.; Bahmanyar, H. Subcritical water gasification of beet-based distillery wastewater for hydrogen production. *J. Supercrit. Fluids* **2015**, *104*, 212−20.
(28) Ptasinski, K. J.; Hamelinck, C.; Kerkhof, P. J. a. M. Exergy analysis of methanol from the sewage sludge process. *Energy Convers. Manage.* **2002**, *43*, 1445−57.
(29) Castello, D.; Rolli, B.; Kruse, A.; Fiori, L. Supercritical Water Gasification of Biomass in a Ceramic Reactor: Long-Time Batch Experiments. *Energies* **2017**, *10*, 1734.
(30) Ma, S.; Tan, Y.; Han, Y. Methanation of syngas over coral reef-like Ni/Al2O3 catalysts. *J. Nat. Gas Chem.* **2011**, *20*, 435−40.
(31) He, C.; Chen, C. L.; Giannis, A.; Yang, Y.; Wang, J. Y. Hydrothermal gasification of sewage sludge and model compounds for renewable hydrogen production: A review. *Renewable Sustainable Energy Rev.* **2014**, *39*, 1127−42.
(32) Gai, C.; Guo, Y.; Liu, T.; Peng, N.; Liu, Z. Hydrogen-rich gas production by steam gasification of hydrochar derived from sewage sludge. *Int. J. Hydrogen Energy* **2016**, *41*, 3363−72.
(33) Kokalj, F.; Arbiter, B.; Samec, N. Sewage sludge gasification as an alternative energy storage model. *Energy Convers. Manage.* **2017**, *149*, 738−47.
(34) Acelas, N. Y.; López, D. P.; Wim Brilman, D. W. F.; Kersten, S. R. A.; Kootstra, A. M. J. Supercritical water gasification of sewage sludge: Gas production and phosphorus recovery. *Bioresour. Technol.* **2014**, *174*, 167−75.
(35) Byrd, A. J.; Pant, K. K.; Gupta, R. B. Hydrogen production from glycerol by reforming in supercritical water over Ru/Al2O3 catalyst. *Fuel* **2008**, *87*, 2956−60.
(36) Wilkinson, N.; Wickramathilaka, M.; Hendry, D.; Miller, A.; Espanani, R.; Jacoby, W. Rate determination of supercritical water gasification of primary sewage sludge as a replacement for anaerobic digestion. *Bioresour. Technol.* **2012**, *124*, 269−75.
(37) Matsumura, Y.; Hara, S.; Kaminaka, K.; Yamashita, Y.; Yoshida, T.; Inoue, S.; et al. Gasification rate of various biomass feedstocks in supercritical water. *J. Jpn. Pet. Inst.* **2013**, *56*, 1−10.

DOI: 10.1021/acs.energyfuels.8b04289
Energy Fuels 2019, 33, 2301−2307